Ubiquitin-Conjugating Enzyme UBE2Q2 Suppresses Cell Proliferation and Is Down-Regulated in Recurrent Head and Neck Cancer

Hiroyuki Maeda,[1,2] Naoto Miyajima,[1] Satoshi Kano,[1,2] Tadasuke Tsukiyama,[1] Fumihiko Okumura,[1] Satoshi Fukuda,[2] and Shigetsugu Hatakeyama[1]

Departments of [1]Biochemistry and [2]Otolaryngology, Head and Neck Surgery, Hokkaido University Graduate School of Medicine, Sapporo, Japan

Abstract

The ubiquitin-proteasome system has a crucial role in maintaining and regulating cellular homeostasis including carcinogenesis. UBE2Q2, also designated Ubci, is one of the ubiquitin-conjugating enzymes (E2), and it has been reported that mRNA of UBE2Q2 is highly expressed in human head and neck squamous cell carcinoma, particularly hypopharyngeal carcinoma. However, the involvement of UBE2Q2 in carcinogenesis has not been fully elucidated. Most cases of head and neck carcinoma are treated with *cis*-diamminedichloroplatinum (II; CDDP) or docetaxel, which are the most effective chemotherapeutic agents against squamous cell carcinomas. Nevertheless, some head and neck cancers develop resistance to these drugs, although the causes and mechanisms remain unknown. In this study, we found high expression levels of UBE2Q2 in human head and neck carcinoma cell lines and cancer tissues by using an anti-UBE2Q2 antibody at the protein level. We also found that the expression level of UBE2Q2 is decreased in cell lines and cancer tissues that have resistance to CDDP or docetaxel and in cancer tissues treated with CDDP or docetaxel. Furthermore, we found that overexpression of UBE2Q2 affects cell proliferation and anchorage-independent cell growth. These findings suggest that UBE2Q2 is a novel oncosuppressor that inhibits tumor growth and is related to the resistance to anticarcinoma agents and that UBE2Q2 likely functions as a novel diagnostic tool and a potentially therapeutic target for head and neck squamous cell carcinoma. (Mol Cancer Res 2009;7(9):1553–62)

Introduction

Head and neck squamous cell carcinoma (HNSCC) is one of most important international health problems. Head and neck carcinoma is the most frequently diagnosed malignancy and is the sixth leading cause of cancer death in humans all over the world (1). HNSCC generally occurs from the mucosa of the upper aerodigestive tract. HNSCC includes cancers of the oral and nasal cavities, the pharynx (nasopharynx, oropharynx, and hypopharynx), the larynx, and the paranasal sinuses. Because the head and neck region includes several different tissues, head and neck cancer contains other kinds of neoplasms such as cancer of the salivary glands and rare histotypes of the paranasal sinuses and thyroid cancer. The major risk factor for head and neck cancer seems to be chronic exposure of epithelial tissues to tobacco smoke and alcohol (2). Environmental factors such as wood and cement dusts and human papillomavirus type 16 and 18 infection are also related to an increased risk of developing HNSCC (3, 4), and EBV infection has been shown to be related to nasopharyngeal squamous cell carcinoma in southern China (5). However, clinical biomarkers for HNSCC management as well as molecular targets for therapy have not been fully elucidated.

Because there has been little improvement in survival rates (6), it is important to uncover the molecular mechanisms involved in HNSCC pathogenesis and to provide new drug targets (7, 8). Recently, it has been reported that cyclin D1 and epidermal growth factor receptor, as well as loss of tumor suppressor genes, are likely to play an important role in the development of HNSCC (9-12). Among the various types of HNSCC, hypopharyngeal carcinoma has the worst prognosis. Almost all cases are differentiated squamous cell carcinoma pathologically. Generally, surgical treatment, irradiation, chemotherapy, and a combination of these treatments are done (6, 13). However, improvement in prognosis of HNSCC is difficult even if combined treatments are used.

Ubiquitination is a versatile post-translational modification mechanism used by eukaryotic cells mainly to control protein levels through proteasome-mediated proteolysis (14). Ubiquitin conjugation is achieved by several enzymes that act in concert, including a ubiquitin-activating enzyme (E1), a ubiquitin-conjugating enzyme (E2), and a ubiquitin-protein ligase (E3; refs. 15-17). UBE2Q2, which has been shown by differential display to be overexpressed in ~85% of hypopharyngeal tumors, can covalently bind ubiquitin on the active site cysteine by thioester formation *in vitro* as an E2 enzyme (18, 19). Human UBE2Q2 protein contains 375 amino acid residues and is characterized by the presence of three functional domains, including a RWD domain, a coiled-coil domain, and an associated UBC domain (20, 21). It has been shown that inactivation of UBE2Q2

Received 11/22/08; revised 6/18/09; accepted 7/6/09; published OnlineFirst 9/1/09.
Grant support: Ministry of Education, Culture, Sports, Science and Technology grant 18076001, Mitsubishi Pharma Sources of Funding, Japan Leukaemia Research Fund, Cell Science Research Foundation, and Uehara Memorial Foundation (S. Hatakeyama).
The costs of publication of this article were defrayed in part by the payment of page charges. This article must therefore be hereby marked *advertisement* in accordance with 18 U.S.C. Section 1734 solely to indicate this fact.
Requests for reprints: Shigetsugu Hatakeyama, Department of Biochemistry, Hokkaido University Graduate School of Medicine, N15, W7, Kita-ku, Sapporo, Hokkaido 060-8638, Japan. Phone: 81-11-706-5899; Fax: 81-11-706-5169. E-mail: hatas@med.hokudai.ac.jp

doi:10.1158/1541-7786.MCR-08-0543

caused a prophase arrest and enhanced caspase-mediated apoptosis in response to microtubule-inhibiting agents (22). These studies have clearly shown that UBE2Q2 has a pivotal function as a positive regulator in cell cycle progression of carcinoma.

It has also been shown that UBE2Q2 is expressed at low-to-undetectable levels in implantation sites of day 6 pregnant endometrium but at high levels in luminal epithelial cells of day 8 pregnant endometrium in the rabbit, indicating that UBE2Q2

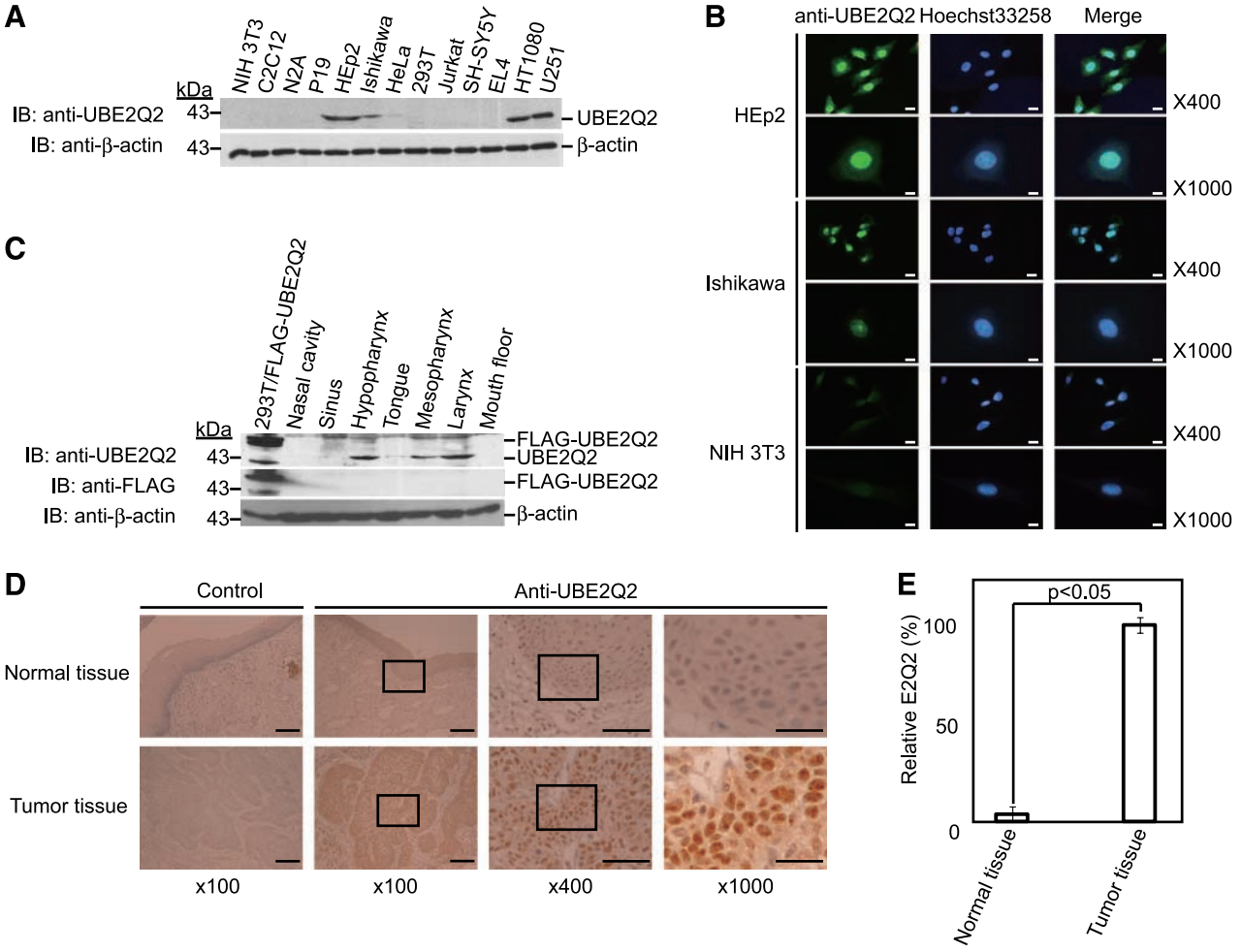

in luminal epithelial cells may play a role in regulating differentiation events through the modification of specific protein substrates in the implantation stage (23).

In this study, to elucidate the molecular function of UBE2Q2 in carcinogenesis, we examined the expression levels of UBE2Q2 in cancer cell lines and tissue samples of HNSCC. We found that overexpression of UBE2Q2 inhibits cell growth and transforming activity. A soft-agar colony formation assay showed that UBE2Q2 has the ability to regulate anchorage-independent growth in collaboration with the active form of c-Src. We also found that expression of UBE2Q2 is reduced by *cis*-diammine-dichloroplatinum (II) (CDDP) or docetaxel in HEp2 cell lines, originating from human laryngeal squamous cell carcinoma. Our results may provide evidence for a direct role of UBE2Q2 in carcinogenesis and resistance to anticancer agents.

Results

Elevated Expression of UBE2Q2 in Human Cell Lines and in HNSCC

It has been reported that expression of UBE2Q2 is elevated in human HNSCC, especially in the hypopharyngeal region (18). We therefore examined the expression levels of UBE2Q2 protein in several human and mouse cancer cell lines and samples of head and neck cancer that had been surgically excised. We established a rabbit polyclonal antibody against human full-length UBE2Q2 that can be used for immunoblot analysis and immunohistochemistry. Immunoblot analysis with the anti-UBE2Q2 antibody showed that UBE2Q2 was expressed at considerably high levels in the human alveolar epithelial carcinoma cell line HEp2, human endometrial cancer cell line Ishikawa, human fibrosarcoma cell line HT1080, and human glioma cell line U251 compared with the levels in other cell lines (Fig. 1A). It has been reported that endogenous UBE2Q2 is expressed mainly in the cytosol and that transfected UBE2Q2 is expressed both in the cytosol and in the nucleus, suggesting that nuclear localization may be a consequence of overexpression (18). To verify subcellular localization of UBE2Q2, we performed immunofluorescent staining using our anti-UBE2Q2 antibody. Endogenous UBE2Q2 was detected mainly in the nuclei and weakly in the cytosol in HEp2 cells, whereas endogenous UBE2Q2 was weakly expressed in Ishikawa cells and was almost undetectable in NIH 3T3 cells (Fig. 1B). To examine the expression levels of UBE2Q2 in several head and neck cancer tissues, immunoblot analysis was done using the anti-UBE2Q2 antibody. Immunoblot analysis showed that UBE2Q2 was remarkably expressed in carcinoma of the hypopharynx and larynx and was moderately expressed in the tongue and mesopharynx (Fig. 1C). We next performed immunohistochemical analysis using squamous cell carcinoma tissues and normal tissues. UBE2Q2 proteins were remarkably detected mainly within the nucleus in tumor cells but also faintly in normal epidermal cells (Fig. 1D), and statistical analysis clarified that UBE2Q2 is expressed at significantly high levels in cancer tissues (Fig. 1E). These results indicate that the expression of UBE2Q2 is elevated in human head and neck carcinoma. To examine the difference between wild-type UBE2Q2 and nonfunctional UBE2Q2, we generated a mutant form of UBE2Q2 in which cysteine 304 is substituted for serine [UBE2Q2 (C304S)]. The stability and subcellular localization of this mutant was examined *in vivo*. Pulse-chase analysis revealed that there was little difference between UBE2Q2(WT) and UBE2Q2(C304S) (Fig. 1F and G). Immunofluorescent staining showed that both UBE2Q2(WT) and UBE2Q2(C304S) mainly localized in the nucleus (Fig. 1H). These findings show that nonfunctional mutation of UBE2Q2 does not affect its stability and subcellular localization.

Expression of UBE2Q2 Is Decreased in CDDP- or Docetaxel-Resistant Variant Cell Lines and Cancer Tissues

The anticancer agents CDDP and docetaxel have been frequently used for treatment of head and neck cancer. Therefore, we examined whether CDDP or docetaxel affects the expression of UBE2Q2 in human HNSCC cell lines. Immunoblot analysis with our anti-UBE2Q2 antibody showed that expression of UBE2Q2 protein was considerably decreased in the antitumor agent–resistant cell lines HEp2/docetaxel and HEp2/CDDP (Fig. 2A). We next performed immunofluorescent staining of UBE2Q2 using the antitumor agent–resistant cell lines HEp2/docetaxel and HEp2/CDDP. In the antitumor agent–resistant cells, UBE2Q2 proteins were also expressed within the nucleus, suggesting that resistance to antitumor agents causes attenuation of UBE2Q2 expression but not change in the subcellular localization of UBE2Q2 (Figs. 1B and 2B). Immunohistochemical analysis with anti-UBE2Q2 antibody was also done using hypopharyngeal squamous cell carcinoma tissues, including normal tissue and CDDP-resistant and docetaxel-resistant HNSCC

FIGURE 1. UBE2Q2 is highly expressed in several cell lines and human HNSCC tissues. **A.** Expression level of UBE2Q2 in several cell lines. Cell lysates from 13 cell lines were subjected to immunoblot analysis with anti-UBE2Q2 antibody. Anti-β-actin antibody was used as a loading control. **B.** Subcellular localization of UBE2Q2 in HEp2, Ishikawa, and NIH 3T3 cells. Immunofluorescence staining was done using anti-UBE2Q2 antibody followed by staining with anti-rabbit IgG-Alexa 546. Hoechst 33258 was used for nuclear staining. Magnification, ×400 and ×1,000. Bar, 25 and 10 μm. **C.** Elevated expression of UBE2Q2 in human HNSCC. Tissue lysates from seven different cancer tissues were subjected to immunoblot analysis with anti-UBE2Q2 antibody. HEK293T transfected with an expression vector encoding FLAG-UBE2Q2 was used as a positive control to verify that anti-UBE2Q2 antibody can exactly react to UBE2Q2. **D.** Immunohistochemical analysis of human hypopharyngeal squamous cell carcinoma tissues with anti-UBE2Q2 antibody. Each sample was surgically resected by total pharyngo-laryngectomy in patients with primary hypopharyngeal squamous cell carcinoma. Normal tissues (*top*) and tumor tissues (*bottom*) were stained with anti-UBE2Q2 antibody. Control was stained with no primary antibody (*left lanes*). Magnification, ×100. Bar, 100 μm. Each black rectangle was magnified at ×400 and ×1,000. Bar, 50 and 20 μm. **E.** Statistical analysis in **D** was done on three tissues in three different fields. The number of stained cells was counted under a microscope. The percentage of stained cells of tumor tissues was defined as 100% and the *P* value was evaluated. Mean ± SD. **F.** Pulse-chase analysis of wild-type and dominant-negative form of UBE2Q2. HEK293T cells were transfected with expression vectors encoding FLAG-UBE2Q2(WT) and FLAG-UBE2Q2(C304S). Forty-eight hours after transfection, the cells were cultured in the presence of cycloheximide (50 μg/mL) for the indicated times. Cell lysates were then subjected to immunoblot analysis with anti-UBE2Q2 and anti-β-actin antibodies. **G.** The intensity of the signals in **F** was normalized by that of the corresponding β-actin and indicated as a percentage of the normalized value at 0 h (*open circle,* WT; *closed circle,* C304S). Mean ± SD of three independent experiments. **H.** Subcellular localization of UBE2Q2 in COS7 cells. COS7 cells were transfected with expression vectors encoding FLAG-UBE2Q2(WT) and FLAG-UBE2Q2(C304S). Immunofluorescence staining was done using anti-FLAG antibody followed by staining with anti-rabbit IgG-Alexa 546. Hoechst 33258 was used for nuclear staining. Magnification, ×400. Bar, 20 μm.

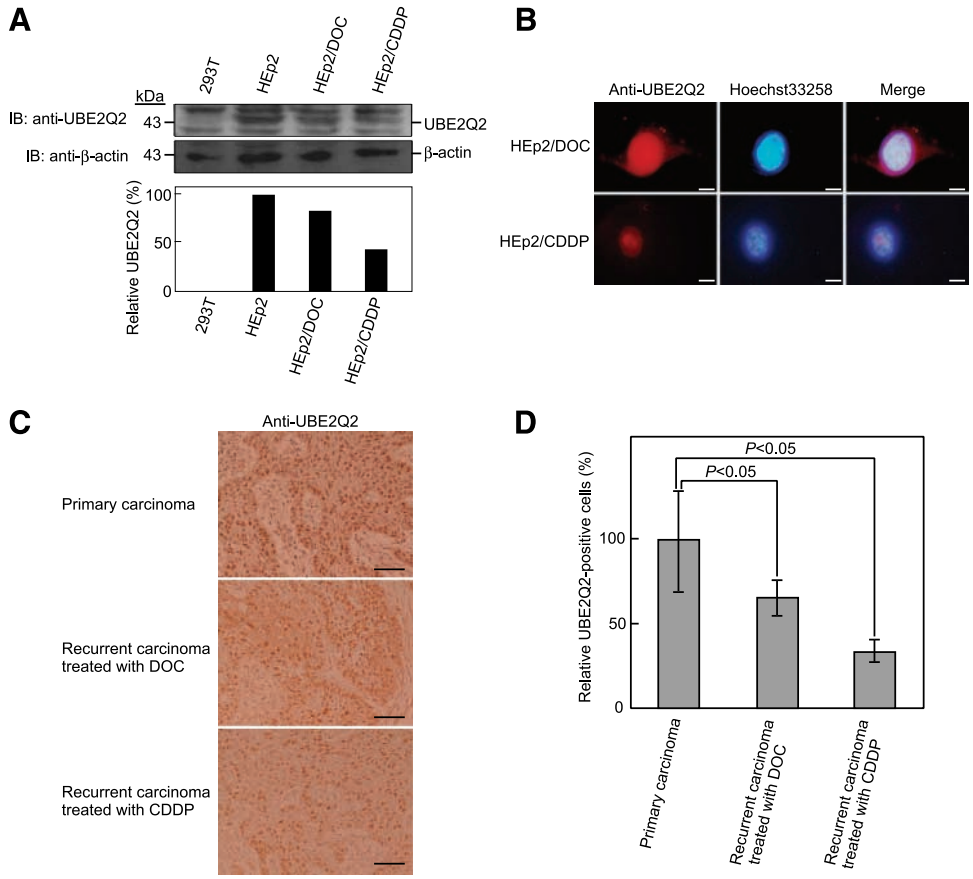

FIGURE 2. Expression of UBE2Q2 is suppressed in antitumor agent–resistant cells and tissues. **A.** Down-regulation of UBE2Q2 in CDDP- or docetaxel-resistant HEp2 cell lines. HEp2 and its CDDP- or docetaxel-resistant variant (HEp2/CDDP and HEp2/docetaxel) cell lines were used for immunoblot analysis with anti-UBE2Q2 antibody. HEK293T was used as a negative control. The intensity of UBE2Q2 bands was normalized by that of the corresponding anti-β-actin bands (*bottom*). The expression level of UBE2Q2 in HEp2 cells was defined as 100%. **B.** Subcellular localization of UBE2Q2 in HEp2/CDDP, and HEp2/docetaxel cell lines. Each cell line was stained with anti-UBE2Q2 antibody. Magnification, ×1,000. Bar, 10 μm. **C.** Immunohistochemical analysis of human hypopharyngeal squamous cell carcinoma tissues in recurrent cancers with anti-UBE2Q2 antibody. Primary cancer tissue, recurrent cancer tissue after treatment with docetaxel (*middle*), and recurrent cancer tissue after treatment with CDDP (*bottom*) were stained with anti-UBE2Q2 antibody. Magnification, ×400. Bar, 50 μm. **D.** Down-regulation of UBE2Q2 in recurrent cancer tissues after treatment with CDDP or docetaxel. The number of stained cells shown in **C** was counted under a microscope. The percentage of stained cells of primary carcinoma was defined as 100% and the *P* value was evaluated. Mean ± SD.

tissues. Immunohistochemical analysis indicated that the number of cells stained with anti-UBE2Q2 antibody and the staining intensity in stained cells were considerably reduced in antitumor agent–resistant hypopharyngeal squamous cell carcinoma tissues compared with those in primary hypopharyngeal squamous cell carcinoma tissues (Fig. 2C). The number of cells stained with anti-UBE2Q2 antibody was counted under a microscope, and it was found that the number of cells stained with anti-UBE2Q2 antibody was significantly reduced in antitumor agent–resistant carcinoma tissues. These findings suggest that the expression level of UBE2Q2 in hypopharyngeal squamous cell carcinoma is affected by treatment with anticancer drugs (Fig. 2D).

Involvement of Expression of UBE2Q2 in Anticancer Drug–Resistant Carcinoma

We next analyzed 45 samples of HNSCC to clarify the relations between number of cells per 1 mm^2 stained with anti-UBE2Q2 antibody and several clinical parameters. The parameters, including age, sex, primary region, clinical stage, pathologic differentiation and treatment, were used for statistical analysis. As reported previously, the numbers of cells stained with anti-UBE2Q2 antibody were significantly larger in hypopharyngeal and mesopharyngeal squamous cell carcinoma tissues than in carcinoma of the tongue, sinus, and other tissues (Fig. 3A). Statistical analysis also showed that the number of cells stained with anti-UBE2Q2 antibody was significantly smaller in cancer tissues treated with chemotherapy than in cancer tissues resected without chemotherapy (Fig. 3B). Age, sex, clinical stage, and pathologic differentiation were not significantly related to the expression level of UBE2Q2 (data not shown). These findings suggest that the expression of UBE2Q2 is increased especially in pharyngeal squamous cell carcinoma but is suppressed after treatment with chemotherapy using CDDP and/or docetaxel.

UBE2Q2 Affects Cell Proliferation

It has been reported that inactivation of UBE2Q2 using a dominant-negative form causes prophase arrest and enhances apoptosis in response to a microtubule-inhibiting agent (22).

To examine the effect of UBE2Q2 on cell proliferation, we established stable NIH 3T3 and HeLa cell lines expressing wild-type UBE2Q2. NIH 3T3 and HeLa cell lines were infected with retroviruses encoding FLAG-UBE2Q2(WT) or an empty vector (Mock). The established NIH 3T3 and HeLa cell lines expressing FLAG-UBE2Q2 (NIH 3T3-FLAG-UBE2Q2 and HeLa-FLAG-UBE2Q2) were checked by immunoblot analysis with anti-FLAG and anti-UBE2Q2 antibodies (Fig. 4A and B). To examine whether UBE2Q2 affects the cell cycle, we synchronized the cells at G_0-G_1 phase by serum starvation and analyzed the time for progression to S phase using established NIH 3T3 cell lines. Flow cytometric analysis and immunoblot analysis showed that UBE2Q2 overexpression causes little change in the cell cycle up to 24 h (Fig. 4C) and that there is little difference in the expression level of UBE2Q2 during different stages of the cell cycle (Fig. 4D). To examine the effect of UBE2Q2 on cell proliferation over a period of time longer than 24 h, stable NIH 3T3 and HeLa cell lines were seeded and harvested to count cell numbers at indicated times. The growth rate of cells with overexpression of UBE2Q2 was markedly decreased compared with that of Mock cell lines (Fig. 4E and F). These results indicate that overexpression of UBE2Q2 likely causes inhibition of cell proliferation.

UBE2Q2 Negatively Regulates Focus Formation and Anchorage-Independent Cell Growth

Because overexpression of UBE2Q2 likely caused inhibition of cell proliferation, we hypothesized that overexpression of UBE2Q2 negatively affects tumorigenesis. We could not find what kind of signal for cell proliferation is related to the function of UBE2Q2 and we tried to use the active form of c-Src (c-SrcY529F) as a oncogene because c-Src is an upstream signal transducer for cell activation. To examine whether expression of UBE2Q2 affects tumorigenicity via c-Src, we established stable NIH 3T3 cell lines expressing UBE2Q2 and the active form of c-Src (c-SrcY529F) by a retroviral expression system. The established NIH 3T3 lines expressing FLAG-UBE2Q2 and c-SrcY529F were checked by immunoblot analysis with anti-FLAG, anti-UBE2Q2, and anti-c-Src antibodies (Fig. 5A). The effect of UBE2Q2 on cell proliferation was confirmed by focus formation assays using these cell lines (Fig. 5B). Many foci were formed by the NIH 3T3 cell line expressing c-SrcY529F, whereas the NIH 3T3 cell line expressing both c-SrcY529F and UBE2Q2 did not form foci, suggesting that UBE2Q2 inhibits the transformation by oncogenic activity of c-SrcY529F. Furthermore, to determine whether UBE2Q2 affects anchorage-independent cell growth by c-Src, a soft-agar colony formation assay was done. The NIH 3T3 cell lines were assayed for their ability to form colonies in soft agar to evaluate their ability to undergo anchorage-independent growth (Fig. 5C). Cells that had not been infected with c-SrcY529F formed few colonies, whereas cells expressing c-SrcY529F formed many colonies. The combination of c-SrcY529F and UBE2Q2 decreased the ability of cells for anchorage-independent growth (Fig. 5D). These findings suggest that UBE2Q2 functions as a negative regulator for anchorage-independent growth in collaboration with c-Src.

Discussion

In this study, we determined the expression levels of UBE2Q2 in cancer cell lines and cancer tissues. We showed that UBE2Q2 is highly expressed in the alveolar epithelial carcinoma cell line HEp2 and in carcinoma of the hypopharynx as reported previously (18). Previous studies have shown high expression of UBE2Q2 in hypopharyngeal tumors mainly at the transcriptional level, whereas we showed high expression of UBE2Q2 in several HNSCC tumors at the protein level (18). Previous studies have shown expression levels of UBE2Q2 in several HNSCC cell lines, whereas we compared the expression levels of UBE2Q2 among several kinds of cancer cell lines, including uterine cancer, lymphoma, and neuroblastoma cell lines (23). We showed high expression levels of UBE2Q2 in the fibrosarcoma cell line HT1080 and glioma cell line U251 as well as in the alveolar epithelial carcinoma cell line HEp2. We also analyzed in detail the expression levels of UBE2Q2 in cancer tissues and showed high

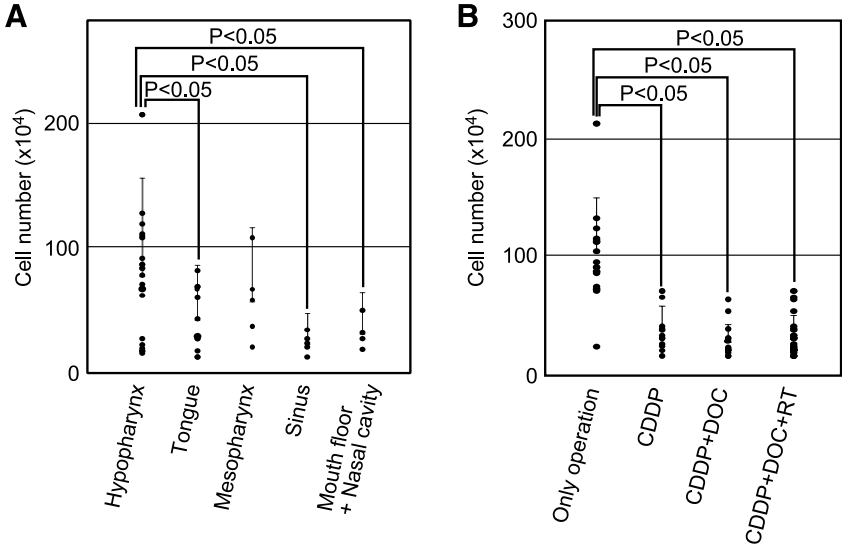

FIGURE 3. Relationships between number of UBE2Q2-positive cells and several clinical scores. UBE2Q2 immunoreactivities were compared in human HNSCC and adjacent normal tissues of 45 cases by immunohistochemistry (Table 1). Mean ± SD. *P* value was calculated by Welch's *t* test. **A.** Number of UBE2Q2-positive cells in each primary cancer region. **B.** Number of UBE2Q2-positive cells in cancer tissues after each treatment. RT, radiation therapy. Mean ± SD. *P* value was calculated.

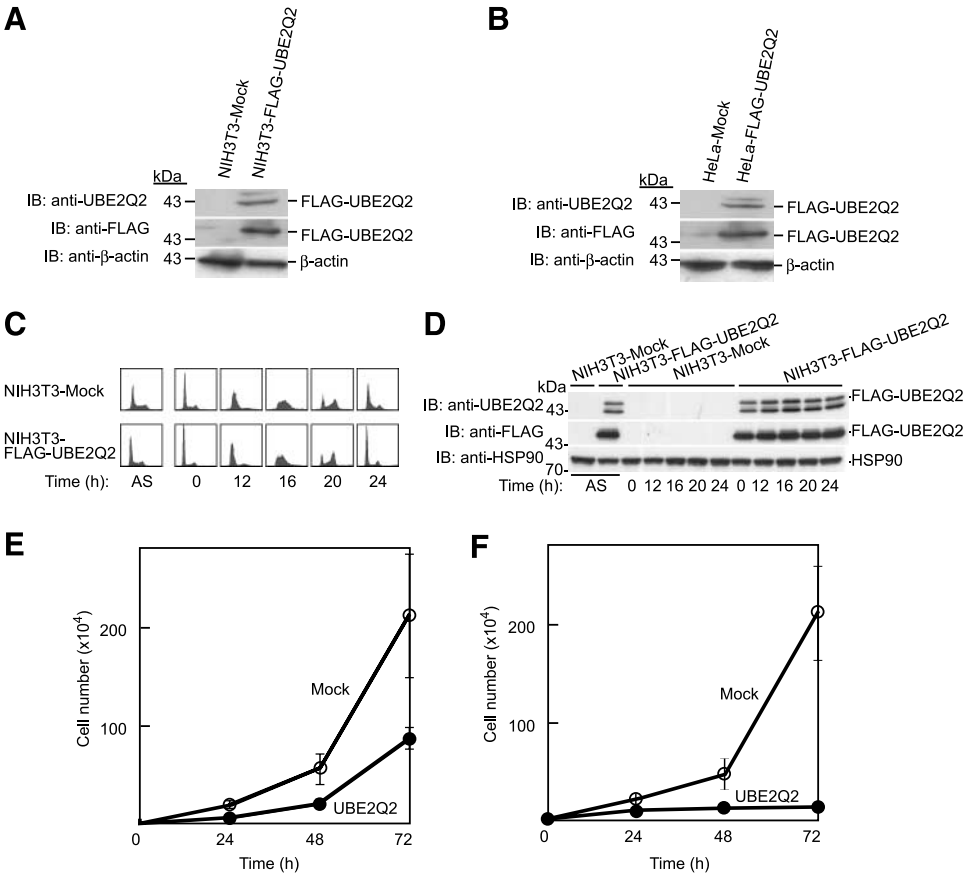

FIGURE 4. Inhibition of cell proliferation by UBE2Q2. **A.** Immunoblot analysis of NIH 3T3 cell lines stably expressing FLAG-tagged UBE2Q2 by using a retroviral expression system. Cell lines were checked by immunoblot analysis using anti-UBE2Q2 and anti-FLAG antibodies. Anti-β-actin antibody was used as an internal control. **B.** Immunoblot analysis of HeLa cell lines stably expressing FLAG-tagged UBE2Q2 by using a retroviral expression system. Cell lines were checked by immunoblot analysis. **C.** Cell cycle analysis of stable NIH 3T3 cell lines expressing FLAG-tagged UBE2Q2 by using a retroviral expression system. Stable NIH 3T3 cell lines were incubated in DMEM with 0.1% calf serum for 24 h for serum starvation. Cells released from serum starvation were harvested at indicated times and then analyzed using a flow cytometer. AS, asynchronous. **D.** Expression level of UBE2Q2 during the cell cycle. NIH 3T3 cells released from serum starvation in **C** were harvested at indicated times and then analyzed using immunoblot analysis with anti-UBE2Q2, anti-FLAG, or anti-HSP90 antibody. HSP90 is shown as a loading control. **E.** Inhibition of cell proliferation by UBE2Q2 in NIH 3T3 cells. NIH 3T3 cells infected with a retrovirus encoding FLAG-UBE2Q2 or the corresponding empty vector (Mock) were seeded at a density of 3×10^3 in 6-well plates and harvested for determination of cell number at indicated times. Mean ± SD of three independent experiments. **F.** Inhibition of cell proliferation by UBE2Q2 in HeLa cells. HeLa cells infected with a retrovirus encoding FLAG-UBE2Q2 or the corresponding empty vector (Mock) were seeded at a density of 3×10^3 in 6-well plates and harvested for determination of cell number at indicated times. Mean ± SD of three independent experiments.

expression levels of UBE2Q2 in cancer tissues of the hypopharynx and larynx and moderate expression levels in the mesopharynx. Previous studies have shown that UBE2Q2 is localized mainly in the cytosol and that overexpression of UBE2Q2 caused nuclear expression as an artifact (18). We established an anti-UBE2Q2 antibody affinity-purified with recombinant UBE2Q2 protein for which specificity was carefully checked. We confirmed nuclear localization of endogenous UBE2Q2 in HEp2 cells and in epithelial cells in normal and malignant hypopharyngeal tissues and showed that transfected FLAG-UBE2Q2 is also localized mainly in the nucleus by immunofluorescent analysis using an anti-FLAG antibody. Given that UBE2Q2 has no typical nuclear localization signal, an unknown protein may control the localization of UBE2Q2. Therefore, it is important to find UBE2Q2-binding proteins for understanding of the subcellular localization of UBE2Q2.

We investigated the difference between expression levels of UBE2Q2 in HEp2 cells and anticancer drug–resistant derivatives. UBE2Q2 is expressed at low levels in HEp2 cell lines that are resistant to docetaxel or CDDP. UBE2Q2 is highly expressed in hypopharyngeal cancers, but high expression level of UBE2Q2 likely gives rise to susceptibility to anticancer drugs. We also showed that expression of UBE2Q2 is suppressed in cancer tissues treated with anticancer drugs such as CDDP and/or docetaxel compared with its expression in cancer tissues without chemotherapy. It is not clear whether low expression level of UBE2Q2 is an advantage for cell proliferation or resistance to anticancer drugs. It is important to unveil the molecular mechanism of the low expression level of UBE2Q2 in anticancer drug–resistant cell lines (24).

Recently, it has been reported that expression of UBE2Q2, which was designated as UBCi (i for implantation), is changed in the endometrium at implantation (23). UBE2Q2 protein is

highly expressed in luminal, but not in glandular, epithelial cells of implantation sites. During implantation, luminal epithelial cells likely undergo differentiation with reorganization of the cytoskeletal networks in collaboration with invasion of the trophoblast. Involvement of UBE2Q2 in reorganization of the epithelial cytoskeleton may be related to characteristics of human UBE2Q2 as an overexpressed gene in hypopharyngeal tumors and its protein as an interacting target for multiple cytoskeletal proteins (18, 19). Previous analysis using immunoaffinity purification linked to mass spectrometry showed that UBE2Q2 interacts with several cytoskeletal proteins including actin and six actin-binding proteins (22).

Oncogene products, but not an oncosuppressor, should be highly expressed in cancer tissues. In our study, immunohistochemical analysis showed high expression of UBE2Q2 in human HNSCC (Fig. 1) and cell biological analysis showed the possibility that UBE2Q2 is a candidate of oncosuppressors (Fig. 4). Therefore, these findings may cause a confusing hypothesis. As one possible interpretation for these results, UBE2Q2 highly expressed in cancer tissues may function as an inactive form or a dominant-negative form. It is important to analyze gene mutation or single nucleotide polymorphisms of the UBE2Q2 gene using HNSCC samples or cancer cell lines in the future.

Moreover, UBE2Q2 plays an important role in the cellular response to microtubule inhibition, and inactivation of UBE2Q2 causes cells to undergo prophase arrest and apoptosis in M phase, suggesting that UBE2Q2 might promote the development of aneuploidy or malignancy as an oncogene in M phase (22). Because UBE2Q2 inhibition causes mitotic arrest only after treatment with a microtubule inhibitor, it is likely to be related to the function of a mitotic checkpoint rather than

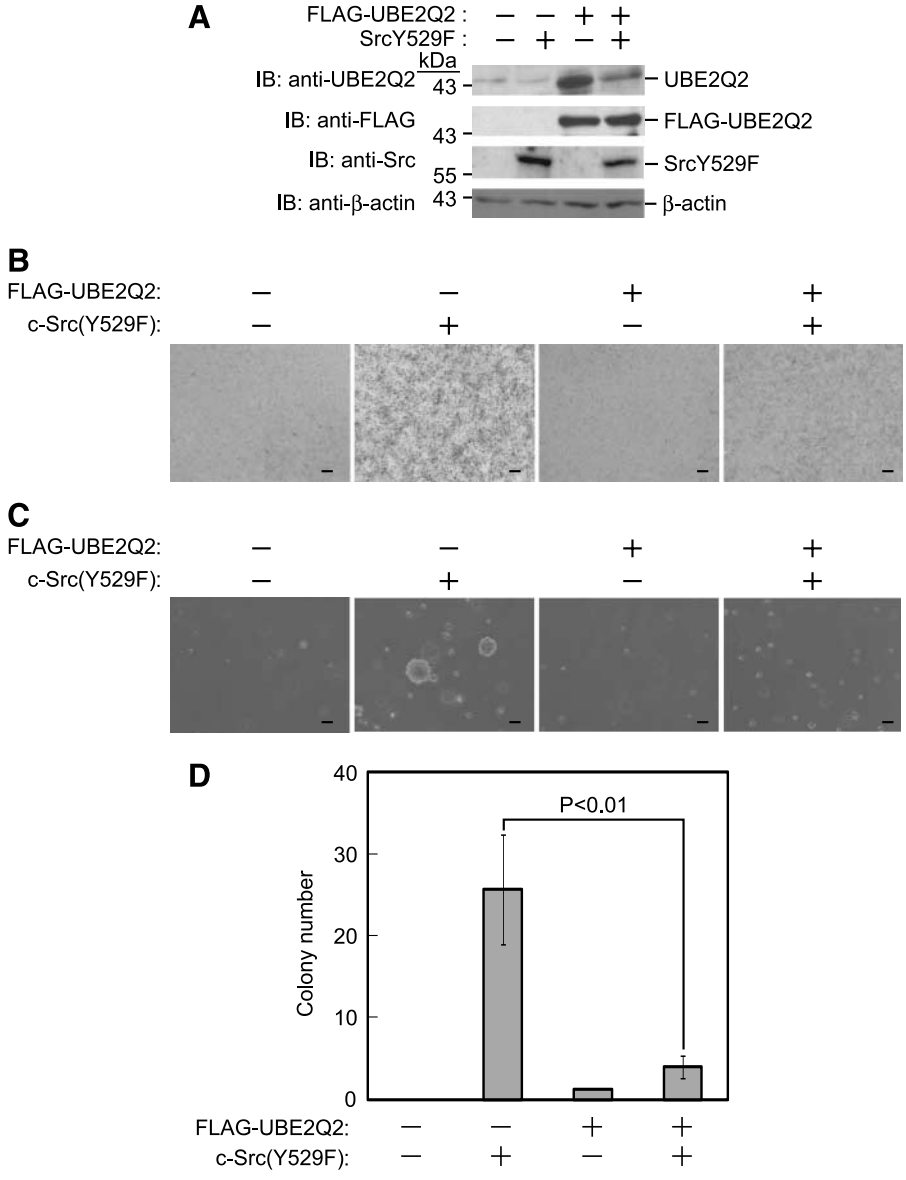

FIGURE 5. UBE2Q2 affects transformation and anchorage-independent cell growth. **A.** NIH 3T3 cells were infected with retroviruses encoding FLAG-UBE2Q2 and/or c-SrcY529F. Cells were checked by immunoblot analysis using anti-UBE2Q2, anti-FLAG, and anti-c-Src antibodies. Anti-β-actin antibody was used as an internal control. **B.** Focus formation assay of NIH 3T3 cells infected with retrovirus vectors encoding FLAG-tagged UBE2Q2 and/or c-SrcY529F. Cell lines were plated at a density of 1×10^4 in 60 mm dishes with drug selection. After 2 wk, confluent cells on dishes were stained by crystal violet and focus formation was observed under a microscope. Bar, 0.1 mm. **C.** Colony formation assay of NIH 3T3 cell lines in soft agar. NIH 3T3 cell lines described in **A** were seeded at a density of 1×10^5 cells in 60 mm dishes containing 0.4% soft agar and cultured for 2 wk. Bar, 0.1 mm. **D.** Numbers of colonies with a diameter of >0.1 mm in randomized areas (per 1 cm^2) were counted. Mean ± SD of three independent experiments. *P* values for the indicated comparisons were determined by Student's *t* test.

perturbing normal mitotic regulation. Because UBE2Q2 antagonizes checkpoint function, overexpression of UBE2Q2 might promote the development of aneuploidy or malignancy. UBE2Q2 has actually been shown to be overexpressed in some malignancies. However, in this study, we showed that overexpression of UBE2Q2 negatively regulates cell proliferation and anchorage-independent cell growth, suggesting that UBE2Q2 is a potential tumor suppressor. Previous studies have also shown that there is a slight delay in cells expressing wild-type UBE2Q2 for entry to G_1 phase of the cell cycle compared with control cells after release from a single thymidine block to synchronize the cell cycle (22). This discrepancy in cell growth by wild-type or mutant-type UBE2Q2 may be due to the difference in procedures for establishing stable cell lines. We used a retroviral expression vector to generate a stable cell line overexpressing wild-type UBE2Q2, whereas others have used a plasmid vector and isolated several clones. Cell biological analyses including cell proliferation assay and soft-agar colony formation assay in our study likely indicate the effects of UBE2Q2 in cell proliferation mainly in early cell cycle stages including G_1 or G_1-S phase. Hence, UBE2Q2 may have different functions according to cell cycle stage. It may be important to fine-tune the expression level of UBE2Q2 for appropriate cell regulation. Moreover, we showed that expression of UBE2Q2 is attenuated in recurrent cancer, suggesting that down-regulation of UBE2Q2 is advantageous for cancer cell growth. Hence, analysis by a genetic approach using transgenic or knockout mice is needed to determine whether UBE2Q2 inhibits cell proliferation. In conclusion, UBE2Q2 likely functions as a negative mediator affecting tumor growth and resistance to CDDP. Results of further studies on UBE2Q2 may be useful for establishing new chemotherapy for head and neck carcinoma.

Materials and Methods

Cell Culture

HEK293T, HeLa, Ishikawa, COS7, HEp2, and its CDDP- or docetaxel-resistant variant (HEp2/CDDP and HEp2/docetaxel) cell lines were cultured under an atmosphere of 5% CO_2 at 37°C in DMEM (Sigma) supplemented with 10% FCS (Invitrogen). HEp2 and HEp2/CDDP cells were provided by Nippon Kayaku. HEp2/docetaxel cells were provided by Dr. T. Mizumachi (Hokkaido University; ref. 25). NIH 3T3 cells were cultured under the same conditions in DMEM supplemented with 10% calf serum (Camblex).

Cloning of cDNAs and Plasmid Construction

Human UBE2Q2 cDNA was amplified from HeLa cDNA (Clontech Laboratories) by PCR with BlendTaq (Toyobo) using the following primers: 5′-AAGATGTCCGTGTCAGGGCTCAAG-3′ (UBE2Q2-sense) and 5′-TATTTAGCCATCTTCCTTTGGAGG-3′ (UBE2Q2-antisense). The amplified fragments were subcloned into pBluescript II SK^+ (Stratagene). UBE2Q2 cDNA was then subcloned into pCR with a FLAG tag (Invitrogen) or pcDNA3 (Invitrogen) for expression in eukaryotic cells, into pET30a (Novagen) for the production of His_6-tagged fusion protein, and into pGEX-6P1 (Amersham Bioscience) for the production of Glutathione *S*-transferase–tagged fusion protein. A dominant-negative form of UBE2Q2 was constructed by replacing cysteine with serine at the 304–amino acid residue [UBE2Q2(CS)] by site-directed mutagenesis (Stratagene).

Recombinant Proteins, Antibodies, and Reagents

Glutathione *S*-transferase–tagged UBE2Q2 was expressed in XL-10 Blue cells and then purified by GSH-Sepharose beads (Roche). His_6-FLAG-tagged UBE2Q2 was expressed in *Escherichia coli* strain BL21 (DE3; Invitrogen) and then purified by using ProBond metal affinity beads (Invitrogen). The recombinant UBE2Q2 protein was used as immunogen in two rabbits. A rabbit polyclonal anti-UBE2Q2 antibody was affinity-purified using a recombinant UBE2Q2-conjugated Sepharose 4B column.

Transfection and Immunoblot Analysis

HEK293T cells were transfected by the calcium phosphate method. After 48 h, the cells were lysed in a solution containing 50 mmol/L Tris-HCl (pH 7.4), 150 mmol/L NaCl, 1% NP-40, 10 μg/mL leupeptin, 1 mmol/L phenylmethylsulfonyl fluoride, 400 μmol/L Na_3VO_4, 400 μmol/L EDTA, 10 mmol/L NaF, and 10 mmol/L sodium pyrophosphate. The cell lysates were centrifuged at 16,000 × *g* for 10 min at 4°C. Immunoblot analysis was done with the following primary antibodies: anti-FLAG (1 μg/mL; Sigma), anti-UBE2Q2 (2 μg/mL; rabbit polyclonal), anti-Src antibody (Upstate), anti-HSP90 (1 μg/mL; Becton Dickinson), or anti-β-actin (1 μg/mL; Sigma). Immune complexes were detected with horseradish peroxidase–conjugated antibodies to mouse or rabbit IgG (1:10,000 dilution; Promega) and an enhanced chemiluminescence system (Amersham).

Establishment of Stable Transfectants by Using a Retroviral Expression System

FLAG-UBE2Q2(WT) or c-SrcY529F cDNA was subcloned into pMX-puro or pMX-hyg, respectively, which were kindly provided by T. Kitamura (University of Tokyo; ref. 26). For retrovirus-mediated gene expression, HeLa cells transfected with mCAT1 (27) and NIH 3T3 cells were infected with retroviruses produced by Plat-E packaging cells and then cultured in the presence of puromycin (2 μg/mL) and/or hygromycin B (0.2 mg/mL; Sigma).

Pulse-Chase Analysis with Cycloheximide

Transiently transfected HEK293T cells were cultured with cycloheximide at the concentration of 50 μg/mL and then incubated for various times. Cell lysates were then subjected to SDS-PAGE and immunoblot analysis with an antibody to UBE2Q2 or β-actin.

Cell Cycle Analysis

NIH 3T3 cells (Mock) and NIH 3T3 cells transfected with FLAG-UBE2Q2 were incubated in DMEM with 0.1% calf serum for 24 h for serum starvation. The cells released from serum starvation were harvested at indicated times and suspended in a solution containing 20 mmol/L HEPES, 160 mmol/L NaCl, 1 mmol/L EGTA, and 0.04% digitonin. The cells were incubated at 37°C for 1 h in a solution with RNase A (100 μg/mL; Novagen) and propidium iodide (20 μg/mL) and then analyzed

with a FACSCalibur flow cytometer and Cell Quest software (Becton Dickinson).

Cell Proliferation Assay

NIH 3T3 and HeLa cell lines were plated into 6-well plates at 3×10^3 cells per well, cultured for the indicated periods, and then counted.

Focus Formation Assay

NIH 3T3 cells infected by a retroviral vector encoding FLAG-UBE2Q2 and/or c-SrcY529F were plated at a density of 1×10^4 in 60 mm dishes and cultured in the presence of puromycin (2 μg/mL) and/or hygromycin B (0.2 mg/mL; Sigma). After 2 weeks, confluent cells on dishes were stained by crystal violet and focus formation was observed under a microscope.

Colony Formation Assay in Soft Agar

Stable NIH 3T3 cell lines were plated at a density of 1×10^5 in 60 mm dishes containing 0.4% top low-melting agarose and 0.5% bottom low-melting agarose medium. Colonies with a diameter of >0.1 mm were counted after 3 weeks.

Human Tissue Samples

Patients with HNSCC who gave informed consent were selected for this study (Table 1). Tumor and surrounding uninvolved mucosa samples in the same patient were removed during surgery and subjected to immunoblot analysis and immunostaining with anti-UBE2Q2 antibody. Clinical stages were determined by tumor-node-metastasis classification (International Union Against Cancer, 6th edition).

Immunohistochemical Analysis

The tissue sections were subjected to immunohistochemical staining with an antibody to UBE2Q2 by a streptavidin-biotin immunoperoxidase method using an immunohistochemical detection kit (Vectastain Elite; Vector) and diaminobenzidine as a chromogen (Wako) according to the manufacturer's instructions. Immunoreactivity was semiquantitatively classified. Two independent investigators reviewed and counted the

Table 1. Clinical Data of Samples Used in this Study

No.	Age	Sex	Primary Region	Clinical Stage	Pathologic Differentiation	Chemotherapy
1	56	F	Hypopharyngo-larynx	I	Well	No
2	61	M	Hypopharyngo-larynx	II	Well	No
3	78	M	Hypopharyngo-larynx	IV	Well	No
4	72	M	Hypopharyngo-larynx	IV	Moderately	No
5	64	M	Hypopharyngo-larynx	II	Moderately	No
6	62	M	Hypopharyngo-larynx	II	Well	No
7	60	M	Hypopharyngo-larynx	II	Well	No
8	55	M	Hypopharyngo-larynx	II	Moderately	No
9	51	M	Hypopharyngo-larynx	III	Poorly	No
10	53	M	Hypopharyngo-larynx	III	Well	No
11	58	M	Hypopharyngo-larynx	IV	Well	No
12	68	M	Hypopharyngo-larynx	III	Well	No
13	63	M	Hypopharyngo-larynx	III	Moderately	No
14	65	M	Hypopharyngo-larynx	III	Well	No
15	68	F	Hypopharyngo-larynx	III	Well	CDDP
16	66	F	Hypopharyngo-larynx	IV	Poorly	CDDP
17	70	M	Hypopharyngo-larynx	III	Well	CDDP
18	73	F	Hypopharyngo-larynx	III	Moderately	CDDP
19	38	M	Hypopharyngo-larynx	IV	Well	CDDP + docetaxel
20	45	M	Hypopharyngo-larynx	IV	Well	CDDP + docetaxel
21	43	F	Hypopharyngo-larynx	IV	Well	CDDP + docetaxel
22	56	M	Hypopharyngo-larynx	IV	Moderately	CDDP + docetaxel
23	46	M	Hypopharyngo-larynx	IV	Moderately	CDDP + docetaxel
24	73	M	Tongue	II	Well	No
25	84	F	Tongue	III	Well	No
26	78	M	Tongue	I	Well	No
27	72	F	Tongue	II	Moderately	CDDP
28	68	M	Tongue	II	Well	CDDP
29	58	M	Tongue	I	Well	CDDP
30	55	F	Tongue	III	Well	CDDP
31	53	M	Tongue	IV	Well	CDDP
32	60	M	Tongue	IV	Well	CDDP + docetaxel
33	71	M	Tongue	III	Well	CDDP + docetaxel
34	79	M	Tongue	III	Well	CDDP + docetaxel
35	60	M	Mesopharynx	IV	Well	No
36	59	M	Mesopharynx	IV	Well	No
37	48	F	Mesopharynx	II	Poorly	CDDP
38	45	M	Mesopharynx	IV	Moderately	CDDP
39	61	M	Sinus	III	Well	CDDP
40	64	M	Sinus	III	Well	CDDP
41	42	M	Sinus	III	Well	CDDP + docetaxel
42	48	F	Sinus	II	Well	CDDP + docetaxel
43	53	M	Mouth floor	IV	Well	CDDP + docetaxel
44	60	M	Mouth floor	IV	Moderately	CDDP + docetaxel
45	63	M	Nasal cavity	IV	Poorly	CDDP + docetaxel

number of cells stained by anti-UBE2Q2 antibody under a microscope.

Statistical Analysis

We used Student's *t* test or unpaired *t* test (Welch's modified method) to determine statistical significance of experimental data.

Disclosure of Potential Conflicts of Interest

No potential conflicts of interest were disclosed.

Acknowledgments

We thank Drs. T. Kitamura and K. Hanada for the plasmids and cell lines, Drs. Y. Ishida, K. Fujii, T. Mizumachi, and N. Oridate for technical assistance, and Y. Soida for help in preparing the article.

References

1. Jemal A, Siegel R, Ward E, et al. Cancer statistics, 2008. CA Cancer J Clin 2008;58:71–96.

2. Argiris A, Karamouzis MV, Raben D, Ferris RL. Head and neck cancer. Lancet 2008;371:1695–709.

3. Morshed K, Polz-Dacewicz M, Szymanski M, Polz D. Short-fragment PCR assay for highly sensitive broad-spectrum detection of human papillomaviruses in laryngeal squamous cell carcinoma and normal mucosa: clinico-pathological evaluation. Eur Arch Otorhinolaryngol 2008;265 Suppl 1:S89–96.

4. Giuliano AR, Tortolero-Luna G, Ferrer E, et al. Epidemiology of human papillomavirus infection in men, cancers other than cervical and benign conditions. Vaccine 2008;26 Suppl 10:K17–28.

5. Gullo C, Low WK, Teoh G. Association of Epstein-Barr virus with nasopharyngeal carcinoma and current status of development of cancer-derived cell lines. Ann Acad Med Sing 2008;37:769–77.

6. Kucukzeybek Y, Gorumlu G, Karaca B, et al. Docetaxel and platinum combination chemotherapy in locally advanced or metastatic head and neck cancer. J BUON 2008;13:199–203.

7. Marur S, Forastiere AA. Head and neck cancer: changing epidemiology, diagnosis, and treatment. Mayo Clin Proc 2008;83:489–501.

8. Kano S, Miyajima N, Fukuda S, Hatakeyama S. Tripartite motif protein 32 facilitates cell growth and migration via degradation of Abl-interactor 2. Cancer Res 2008;68:5572–80.

9. Pabalan N, Bapat B, Sung L, et al. Cyclin D1 Pro^{241}Pro (CCND1-G870A) polymorphism is associated with increased cancer risk in human populations: a meta-analysis. Cancer Epidemiol Biomarkers Prev 2008;17:2773–81.

10. Mehra R, Cohen RB, Burtness BA. The role of cetuximab for the treatment of squamous cell carcinoma of the head and neck. Clin Adv Hematol Oncol 2008; 6:742–50.

11. Mehra R, Cohen RB, Harari PM. EGFR inhibitors for the treatment of squamous cell carcinoma of the head and neck. Curr Oncol Rep 2008;10: 176–84.

12. Sattler M, Abidoye O, Salgia R. EGFR-targeted therapeutics: focus on SCCHN and NSCLC. Sci World J 2008;8:909–19.

13. Bernier J. Drug Insight: cetuximab in the treatment of recurrent and metastatic squamous cell carcinoma of the head and neck. Nat Clin Pract Oncol 2008; 5:705–13.

14. Hershko A, Ciechanover A. The ubiquitin system. Annu Rev Biochem 1998; 67:425–79.

15. Scheffner M, Nuber U, Huibregtse JM. Protein ubiquitination involving an E1-E2-E3 enzyme ubiquitin thioester cascade. Nature 1995;373:81–3.

16. Lorick KL, Jensen JP, Fang S, et al. RING fingers mediate ubiquitin-conjugating enzyme (E2)-dependent ubiquitination. Proc Natl Acad Sci U S A 1999;96:11364–9.

17. Hatakeyama S, Yada M, Matsumoto M, Ishida N, Nakayama KI. U box proteins as a new family of ubiquitin-protein ligases. J Biol Chem 2001;276: 33111–20.

18. Seghatoleslam A, Zambrano A, Millon R, et al. Analysis of a novel human gene, LOC92912, over-expressed in hypopharyngeal tumours. Biochem Biophys Res Commun 2006;339:422–9.

19. Melner MH, Haas AL, Klein JM, et al. Demonstration of ubiquitin thiolester formation of UBE2Q2 (UBCi), a novel ubiquitin-conjugating enzyme with implantation site-specific expression. Biol Reprod 2006;75:395–406.

20. Nameki N, Yoneyama M, Koshiba S, et al. Solution structure of the RWD domain of the mouse GCN2 protein. Protein Sci 2004;13:2089–100.

21. Carbia-Nagashima A, Gerez J, Perez-Castro C, et al. RSUME, a small RWD-containing protein, enhances SUMO conjugation and stabilizes HIF-1α during hypoxia. Cell 2007;131:309–23.

22. Banerjee S, Brooks WS, Crawford DF. Inactivation of the ubiquitin conjugating enzyme UBE2Q2 causes a prophase arrest and enhanced apoptosis in response to microtubule inhibiting agents. Oncogene 2007;26:6509–17.

23. Melner MH, Ducharme NA, Brash AR, Winfrey VP, Olson GE. Differential expression of genes in the endometrium at implantation: upregulation of a novel member of the E2 class of ubiquitin-conjugating enzymes. Biol Reprod 2004;70: 406–14.

24. Higuchi E, Oridate N, Furuta Y, et al. Differentially expressed genes associated with *cis*-diamminedichloroplatinum (II) resistance in head and neck cancer using differential display and cDNA microarray. Head Neck 2003;25:187–93.

25. Mizumachi T, Suzuki S, Naito A, et al. Increased mitochondrial DNA induces acquired docetaxel resistance in head and neck cancer cells. Oncogene 2008;27:831–8.

26. Kitamura T. New experimental approaches in retrovirus-mediated expression screening. Int J Hematol 1998;67:351–9.

27. Hanada K, Kumagai K, Yasuda S, et al. Molecular machinery for non-vesicular trafficking of ceramide. Nature 2003;426:803–9.